

Z.R. Zapukhlyak<sup>1</sup>, L.I. Nykyruy<sup>1</sup>, V.M. Rubish<sup>2</sup>, G. Wisz<sup>3</sup>, V.V. Prokopiv<sup>1</sup>,  
M.O. Galushchak<sup>4</sup>, I.M. Lishchynskyy<sup>1</sup>, L.O. Katanova<sup>1</sup>, R.S. Yavorskyi<sup>1</sup>

## **SCAPS Simulation of ZnO/CdS/CdTe/CuO Heterostructure for Photovoltaic Application**

<sup>1</sup>Vasyl Stefanyk Precarpathian National University, Ivano-Frankivsk, Ukraine, [zhanna.zapukhlyak@gmail.com](mailto:zhanna.zapukhlyak@gmail.com)

<sup>2</sup>Uzghorod Laboratory of Institute for Information Recording of NAS of Ukraine, Uzghorod, Ukraine, [center.uzh@gmail.com](mailto:center.uzh@gmail.com)

<sup>3</sup>Rzesow University, Rzesow, Poland, [gwisz@ur.edu.pl](mailto:gwisz@ur.edu.pl)

<sup>4</sup>Ivano-Frankivsk National Technical University of Oil and Gas, Ivano-Frankivsk, Ukraine, [galuschak@nung.edu.ua](mailto:galuschak@nung.edu.ua)

In the computer simulations environment of photoelectric cells SCAPS (Solar Cell Capacitance Simulator) complex modeling of optical and photoelectric properties of the cell based on the heterostructure ZnO/CdS/CdTe/CuO was performed. The choice of highly resistive transparent (HRT) oxide material - for use as a front contact is justified. The influence of film thickness on the efficiency of the final cell is investigated. The efficiency of the considered photovoltaic cell was 20.94%. The structure of the photovoltaic cell was chosen based on the analysis of the properties of individual layers with a certain thickness from a pre-selected range. In this case the properties of the heterosystem were reviewed each time with adding each subsequent layer. Thus, the optimal thicknesses for the photoelectric heterosystem are selected, which allow to obtain the maximum efficiency. The simulation was based on experimental data (thickness, optical characteristics, band gap) for each of the films obtained by physical vapor deposition (PVD).

**Key words:** thin films, photoelectricity, CdTe, ZnO/CdS/CdTe/CuO heterostructure, solar cells, SCAPS modeling.

*Received 23 September 2020; Accepted 15 December 2020.*

### **Introduction**

By the beginning of the 21<sup>st</sup> century, the market share of silicon batteries was over 99.8%, and over the last 20 years it has decreased by 22.8%, and continues to decline rapidly. Instead, 2nd generation photovoltaic converters based on the thin film technologies appeared, which have already demonstrated competitiveness with silicon analogues. Thin-film solar panels have a lower weight of ~ 20-25%, increased efficiency and much better functionality.

The most promising materials on the basis of which it is possible to obtain high-effective thin-film photovoltaic cells are II-VI based compounds, in particular, CdTe, CdS [1- 3].

Solar cells based on CdTe are one of the most promising representatives for photovoltaic energy conversion in recent years [4, 5], which can reach the maximum value of the possible theoretical efficiency of approximately 28% -30% [6] (Fig. 1). To improve the

efficiency of thin-film photovoltaic systems, heterostructures are created on the basis of above mentioned materials [7], where CdTe is an active part of the solar cell, where the largest generation and accumulation of carriers occurs. The CdS is a strong absorber of light [8, 9]. However, it should be noted that light absorbed in this layer is wasted because carriers photogenerated in CdS are not collected.

The record efficiency of 12.8% [10] in 2011 of laboratory size CdTe thin-film solar cells on glass substrates has dramatically improved to 18.3% [11] in 2020 and for single-junction CdTe terrestrial cells the record efficiency values are 16.7% and 21.0% respectively. The recent rapid increase in cell efficiency is due to the enhancements of the short circuit current ( $J_{sc}$ ) in the short-wavelength regions [12]. First Solar (USA): is the largest worlds PV SCs manufacturer and has the best industrial technology for production of CdTe-based SC on glass substrate [5].

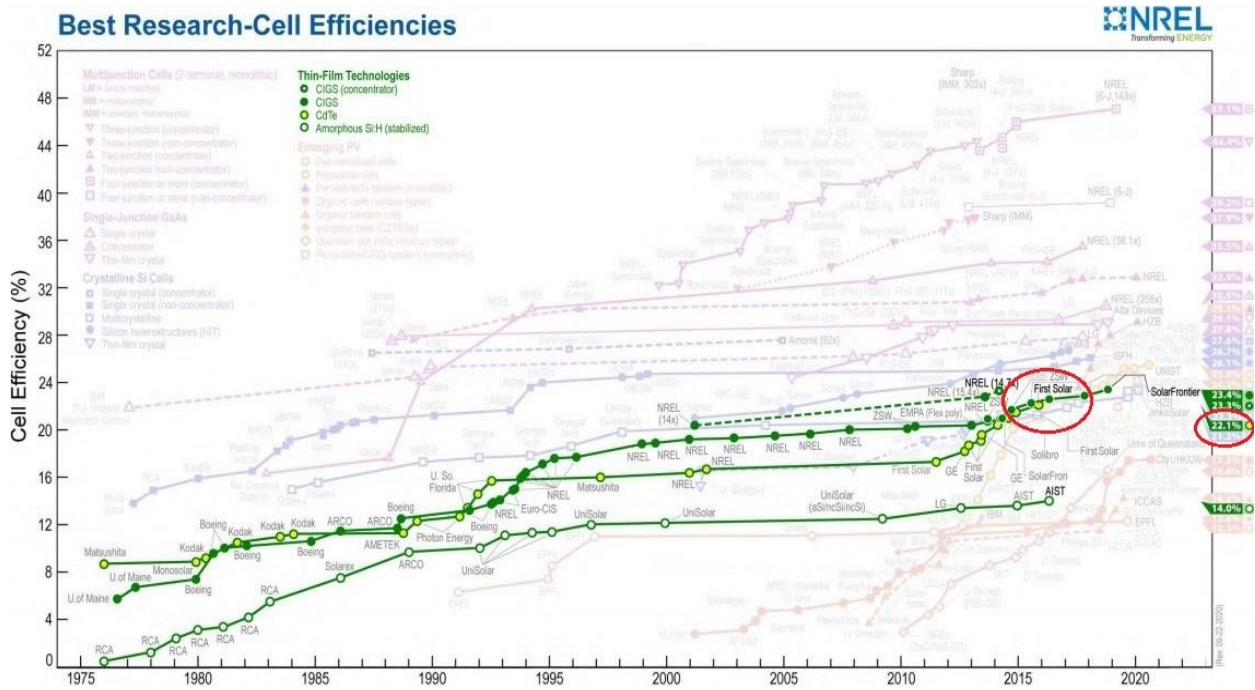


Fig. 1. Звіт NREL: Діаграма найкращих досліджень ефективності сонячних комірок [5].

A variety of studies on the device modeling of CdTe solar cells using the SCAPS simulation method, has been reported previously [13-15] and discussed how some material parameters impact the characteristics of CdTe thin film solar cells [16].

The authors of this paper developed a simple, cheap and reproducible technology for obtaining thin-film heterostructures CdS/CdTe with a given surface morphology during open evaporation in vacuum, which allows to obtain homogeneity of the base layer for better absorption of solar radiation and contributes to their low cost [17, 18]. It was obtained an efficiency of 15.8% for deposited CdS/CdTe heterostructure on glass substrate [19].

Considering thin films are relatively new systems, their study can offer much wider opportunities for technological improvement of photovoltaic energy converters. Therefore the numerical simulations of heterojunction thin film solar cells based on CdTe with multilayer structure on glass substrates has been conducted in this paper.

According to the referenced literature [20] the authors examined whether introducing a transparent conductive ZnO layer improves the efficiency of the final heterostructure. For this purpose the appropriate simulations in SCAPS were performed and the authors tried to increase the efficiency of ZnO/CdS/CdTe heterostructure by introducing a CuO layer, in order to substantiate the optimal thickness of individual layers.

## I. Experiment and simulation

Nowadays, it is difficult to analyze measurements without the precise model, therefore the use of computer simulation tools has several advantages.

Numerical simulation is of a great interest for understanding the impact of different physical parameters on cell performance, it minimizes the cost of manufacturing prototypes, it makes it possible to design different solar cells based on crystalline, polycrystalline and amorphous materials [21–22] and offers the opportunity to study the influence of each layer of the cell in the case of interdependent parameters.

Therefore a computer simulation tool was employed in this research to analyze numerically the performances of the designed thin film heterostructures.

Solar Cell Capacitance Simulator - 1 Dimension (SCAPS-1D) is a graphic solar cell simulation program, developed with LabWindows/CVI of National Instruments, at the department of Electronics and Information Systems (ELIS) of the University of Gent in Belgium by Professor Marc Burgelman [23]. A program description and the algorithms that it uses are given in [24–28].

### 1.1. Electrical model

SCAPS-1D is an interactive application for Windows, written in code C, mainly used to model thin-film solar cells based on CdTe, CIS and CIGS and allows to solve one-dimensional semiconductor equations, such as:

a) *current – density equations*: they are also called as constitutive equations. [29] Current conductivity mainly consists of two components: drift and diffusion. Drift component namely is caused by electric field and diffusion component is caused by the carrier-concentration gradient. The equations are:

$$J_n = q\mu_n nE + qD_n \frac{dn}{dx} = q\mu_n \left( nE + \frac{kT}{q} \frac{dn}{dx} \right) = \mu_n n \frac{dE_{Fn}}{dx} \quad (1)$$

$$J_p = q\mu_p pE + qD_p \frac{dp}{dx} = q\mu_p \left( pE + \frac{kT}{q} \frac{dp}{dx} \right) = \mu_p p \frac{dE_{Fp}}{dx} \quad (2)$$

where,  $\varepsilon$  – relative permittivity,  $\mu_n, \mu_p$  – electron and hole mobility respectively;  $J_n, J_p$  – electron and hole current density respectively;  $D_n, D_p$  – diffusion coefficient for electrons and holes respectively;  $E_{Fn}, E_{Fp}$  – quasi-Fermi level for electron and hole respectively.

b) *continuity equations*: in a semiconductor there are different mechanisms of carrier transport, so the continuity equations take into account time-dependent phenomena, such as generation, recombination and low-level injection. The effect of drift, diffusion, indirect or direct thermal generation or recombination leads to a change in the concentration of carriers over time. The net change in carrier concentration is the difference between generation and recombination, plus the net current flowing in and out of that region. That is, the continuity equation is basically the equation of conservation of carrier currents:

$$-\frac{\partial J_n}{\partial x} - U_n + G = \frac{\partial n}{\partial t} \quad (3)$$

$$-\frac{\partial J_p}{\partial x} - U_p + G = \frac{\partial p}{\partial t} \quad (4)$$

where,  $G$  – generation rate;  $U_n, U_p$  – net recombination/generation rate.

c) *Poisson equation*: gives a starting point for obtaining a qualitative solution for electrostatic variables in a semiconductor. It mainly concerns the distribution of the electric field inside the device. This simulation can be considered as a time-independent analysis, so the basic equation can be presented accordingly:

$$\frac{\partial}{\partial x} \left( \varepsilon_0 \varepsilon \frac{\partial \psi}{\partial x} \right) = -q(p - n + N_D - N_A) \quad (5)$$

where  $\varepsilon$  – relative permittivity,  $q$  – elementary charge,  $q(p - n + N_D - N_A) = \rho$  (charge density), considering the dopants to be fully ionized,  $N_D, N_A$  - Ddnor and acceptor impurity concentration respectively.

Together with the corresponding boundary conditions on the interfaces and contacts, this leads to the creation of a system of differential equations ( $\Psi, n, p$ ) або ( $\Psi, E_{Fn}, E_{Fp}$ ).

For interface recombination, SCAPS-1D uses the Pauwells Vanhoutte model [24], which considers four bands for interface states, i.e. the conduction and valence bands of both semiconductors on the interface.

This theory considers the recombination of electrons of one semiconductor with holes in another semiconductor together with the standard recombination of electrons with holes within the same semiconductor (Fig. 2). The most important recombination path is the recombination of "window electrons" with "absorber holes". The total charge in the interface states is equal to the discontinuity in the dielectric displacement at the interface.

SCAPS-1D provides that quasi-level electrons of electrons and holes are interrupted at the interface when current flows through the interface. This is taken into account by including one additional node on the interface in the numerical algorithm. The electrostatic potential is assumed continuous at the interfaces.

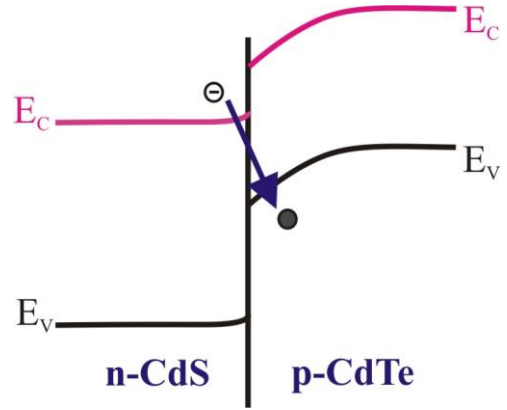


Fig. 2. Model of CdS/CdTe heterojunction [24].

### 1.2. Optical model

Optical characteristics of thin films provide information about physical properties, for example. band gap and optically active defects, etc. Spectral distribution of optical transparency was performed to identify thin films of CdTe, CdS and ZnO [20]. The region of the main absorption was observed in the transmission spectra. The transmission spectra of thin films obtained on glass substrates with different film thicknesses were measured in the wavelength range 180 nm - 1500 nm and (180 - 3200) nm and are shown in Fig. 3 (a).

Fig. 3 (b) shows the dependence  $(\alpha h\nu)^2 - h\nu$  obtained by the Tauk formula [17]. The band gap is estimated by extrapolation from the intersection of the linear part at  $\alpha = 0$ . The optical band gap of CdTe thin films was  $\sim 1.48$  eV. The spectral dependence of absorption for CdS films on the graph shows the presence of a fundamental absorption limit ( $E_g = 2.38$  eV).

For ZnO thin films, the absorption edge is about 350 nm for all samples. It can be seen that thin films show transparency in the visible range of average transmission, which is between 30% and 70%. The increase in the band gap with increasing substrate temperature is explained as a shift in the electron density of Burstein. The band gap of ZnO films is  $\sim 3.8$  eV

Using the obtained experimental data of the band gap of each layer at a specific film thickness, the measurements of photovoltaic cells were simulated in SCAPS in light under the solar spectrum with an incident solar power of  $P = 1000 \text{ W / m}^2$  at a temperature of 300 K.

### 1.3. Simulation

In this paper was verified whether the introduction of each new layer really affects the efficiency of the final structure. And the principle of work in this study was as follows: to add each subsequent layer of heterostructure, without changing the best value determined for the thickness of the previous layer.

The device structure of CdTe solar cells used in the final simulation consisted of ZnO (TCO) layer, CdS "window layer, CdTe absorber layer and bottom contact CuO is exhibited in Fig. 4. This model is a simplification of the actual cell.

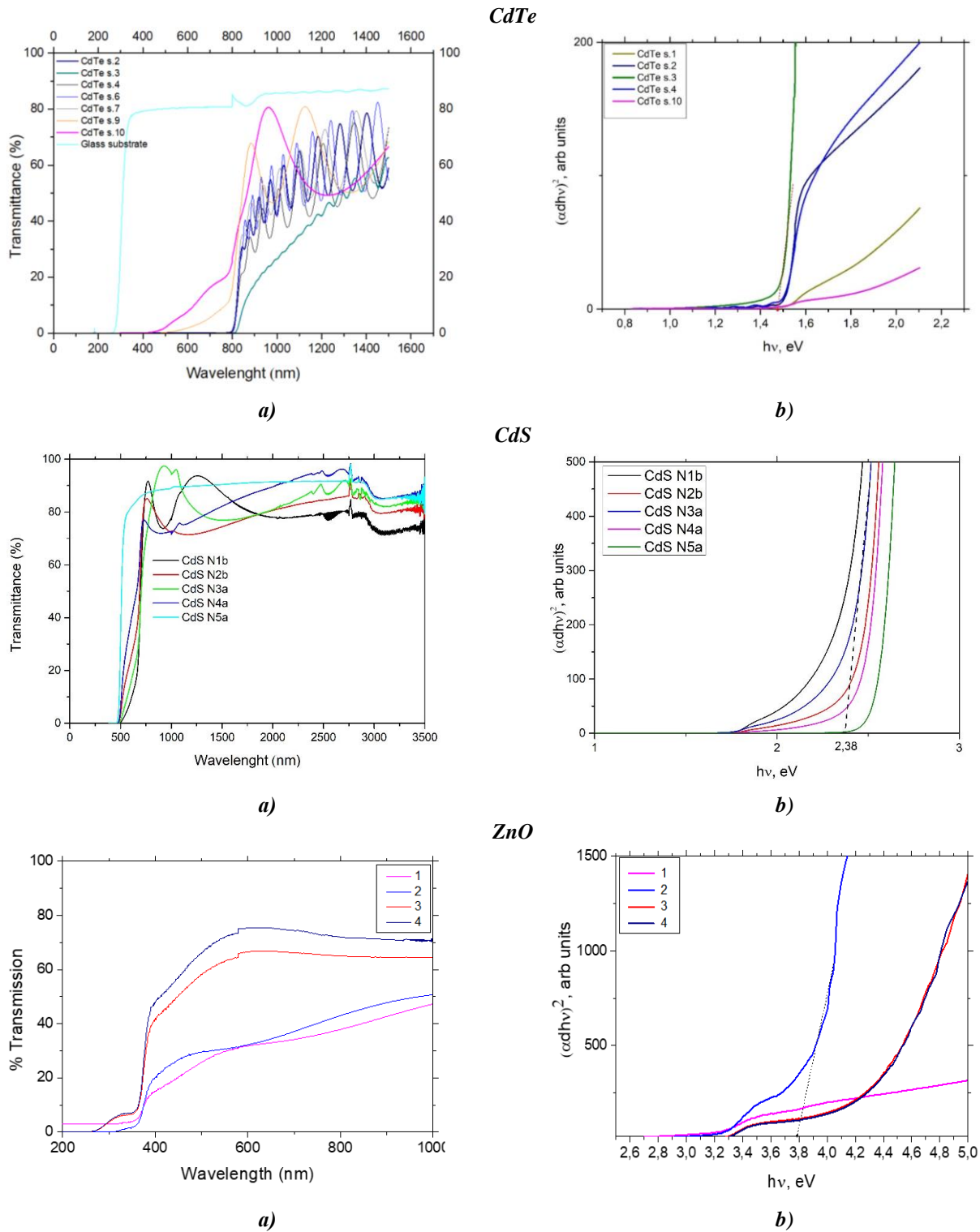


**Fig. 3.** Optical transmission (a) and band gap (b) of thin films (CdTe, CdS, ZnO)/glass.

To proceed with the simulations, the majority of input parameters were mainly selected based on the reported literature values [19, 20, 30-36] or estimated in a reasonable ranges and are shown in Table 1.

The main screen that appears after running SCAPS-1D is shown in Fig. 5. Dashboard contains a series of operations and user can get simulation results in the form of following characteristics: I-V, C-V, C-f,  $Q(\lambda)$ , electric

field, band diagrams, carrier densities, partial recombination currents. In SCAPS software the parameters of materials and an operating point can be set: temperature, voltage, frequency and illumination.

Fig. 6 shows the SCAPS solar cell definition panel, where specific parameters for each layer can be set. The material properties of each layer were selected from Table 1.



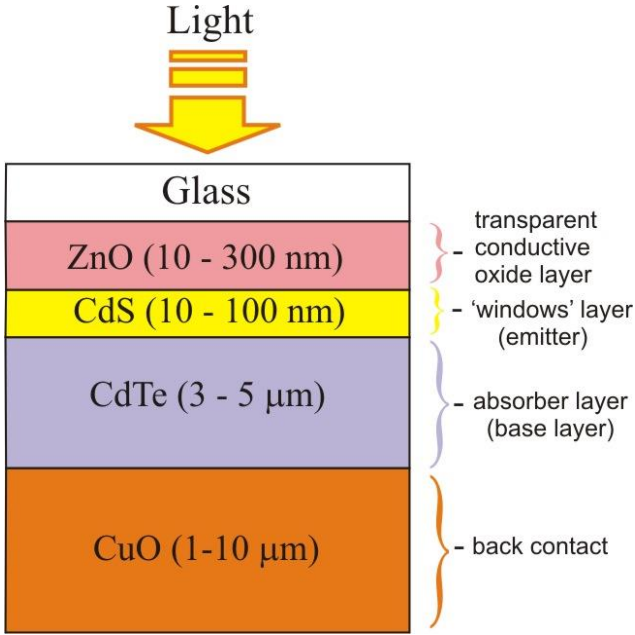


**Fig. 4.** Device structure of CdTe solar cells for the final devices simulations

**Table 1.**

Material parameters used for simulation in SCAPS environment [19, 20, 30-36]

Parameters	Values			
	CuO	CdTe	CdS	ZnO
Thickness, μm	1,0-10,0	3,0-5,0	0,01-0,1	0,01-0,1
Bandgap, eV	1,51	1,5	2,4	3,3
Electron affinity, eV	4,07	3,9	4,0	4,6
Dielectric permittivity (relative)	18,1	9,4	10,0	9,0
CB effective density of states, cm <sup>-3</sup>	2,2 · 10 <sup>19</sup>	8,0 · 10 <sup>17</sup>	2,2 · 10 <sup>18</sup>	2,2 · 10 <sup>18</sup>
VB effective density of states, cm <sup>-3</sup>	5,5 · 10 <sup>20</sup>	1,8 · 10 <sup>19</sup>	1,8 · 10 <sup>19</sup>	1,8 · 10 <sup>19</sup>
Electron mobility, cm <sup>2</sup> /(V·s)	1,0 · 10 <sup>2</sup>	3,2 · 10 <sup>2</sup>	1,0 · 10 <sup>2</sup>	1,0 · 10 <sup>2</sup>
Hole mobility, cm <sup>2</sup> /(V·s)	0,1	40	25	25
Electron thermal velocity (cm/s)	1,0 · 10 <sup>7</sup>	1,0 · 10 <sup>7</sup>	1,0 · 10 <sup>7</sup>	1,0 · 10 <sup>7</sup>
Hole thermal velocity (cm/s)	1,0 · 10 <sup>7</sup>	1,0 · 10 <sup>7</sup>	1,0 · 10 <sup>7</sup>	1,0 · 10 <sup>7</sup>
N <sub>D</sub> , cm <sup>-3</sup>		0	1,1 · 10 <sup>18</sup>	1,1 · 10 <sup>18</sup>
N <sub>A</sub> , cm <sup>-3</sup>	1,0 · 10 <sup>16</sup>	2,0 · 10 <sup>14</sup>	0	0

The conversion efficiency of solar radiation into photoelectric energy is determined by the width of the band gap of the studied heterostructure. SCAPS simulation tool allows to build appropriate band diagrams.

In the present contribution, J-V dependence was used to characterize thin film heterostructures. It is the most common tool for solar cell characterizing. In addition to simulated J-V curves, SCAPS shows simultaneously the table of values, among which the efficiency values can be found, at various thicknesses of the variable layer while the thicknesses of the other layers remain unchanged. In particular, the efficiency η was obtained according to the equation:

$$\eta = \frac{I_{sc} \cdot V_{oc} \cdot FF}{P_{in}} \quad (6)$$

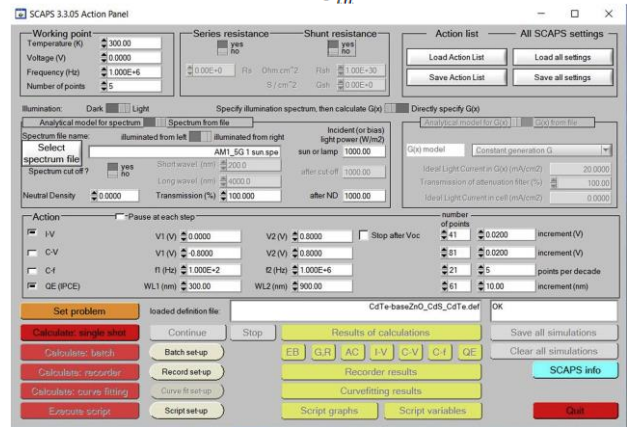


**Fig.5.** SCAPS start-up panel.

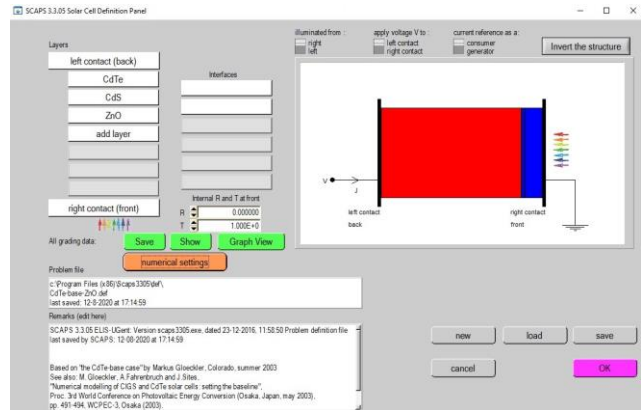


**Fig. 6.** SCAPS definition panel.

## II. Results and discussion

Fig. 7 shows the simulation results for CdS/CdTe heterostructure, where the best CdTe layer thickness was determined and set to 3 μm, while the thickness of CdS layer was varied in the range of 10-100 nm. The efficiency values of 15.87%(system including defects) and 18.08%(defect-free system) were obtained, which is consistent with the results presented in the article [18].

In [18], the influence of technological parameters of PVD deposition on the optical characteristics of thin films was studied. In addition, for CdS/CdTe system, the

optimal thicknesses were determined to achieve the maximum photoelectric efficiency of such a heterostructure as a photoelectric cell. Accordingly, the cell structure of CdTe/CdS type was taken as the baseline for the next stages of modeling in this study. Then, a ZnO (TCO) layer and a back contact layer were gradually added to the designed model.

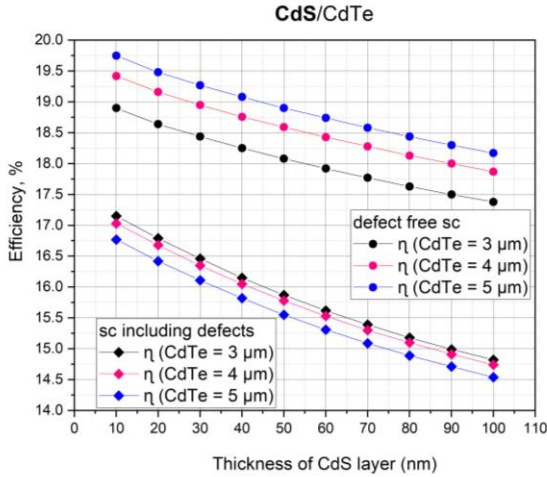


**Fig. 7.** Variation of the efficiency value  $\eta$  for CdS/CdTe heterojunction including defects and defect free SC as a function of CdS window layer thickness ( $d_{CdS}=10-100$  nm).

The next step in this study was to introduce a conductive ZnO layer and to verify the improved efficiency of a new heterostructure.

The simulations for ZnO/CdS/CdTe heterostructure were performed, where CdTe and CdS layer thicknesses were unchanged and set to 3 μm and 50 nm respectively, while the thickness of ZnO layer was varied in the range of 10-100 nm. Fig. 8 shows the simulation results, where the best efficiency values of 15.15% and 18.68% were determined (including and without defects, respectively).

To a greater extent, the efficiency of the final structure of ZnO/CdS/CdTe depends on well-chosen thicknesses of CdS and CdTe layers.

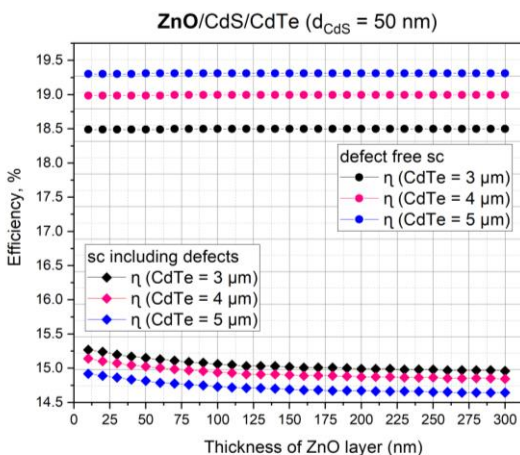


**Fig. 8.** Variation of the efficiency value  $\eta$  for ZnO/CdS/CdTe heterojunction as a function of ZnO transparent conductive oxide layer thickness ( $d_{ZnO}=10-300$  nm).

The use of a high-resistive transparent (HRT) layer between the TCO and the CdS window layer will increase the efficiency by limiting the effect of non-uniformity [35]. Unalloyed tin oxide ( $i-SnO_2$ ) or zinc oxide ( $i-ZnO$ ) are among the materials used as the HRT layer. In the 1980s, there were interesting studies on the back surface field (BSF) and its effect on the efficiency of solar cells [37].

The large band gap of the material is used as a carrier repulsion barrier in the CdTe/BSF heterojunction to minimize carrier losses on the back contact. Moreover, it reduces the recombination of the carriers on the back contact and thus improves the efficiency of the cell. In the same context, studies have shown that the use of the hole transport-electronic blocking layer (HT-EBL) plays the same role as the BSF layer. It also helps to increase the efficiency of the solar cell. A promising materials used as an HT-EBL layer in CdTe solar cells are cuprous oxide ( $Cu_2O$ ) and cupric oxide ( $CuO$ ), which have a large band gap in the range of 2.1 - 2.61 eV and ~ 1.51 eV and p-type conductivity [38,39].

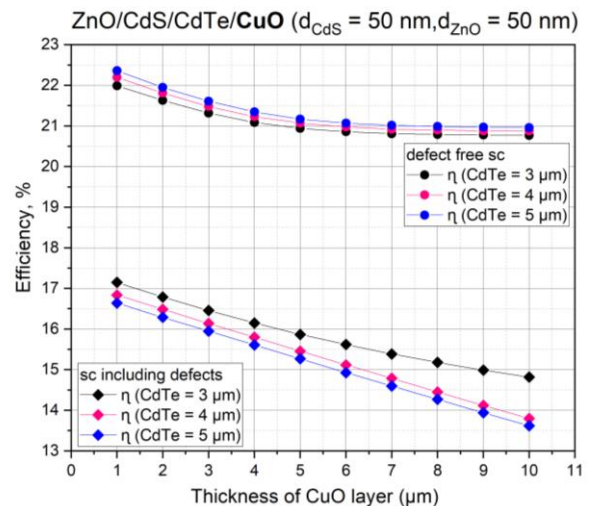


**Fig. 9.** Variation of the efficiency value  $\eta$  for ZnO/CdS/CdTe/CuO heterojunction as a function of CuO contact layer thickness ( $d_{CuO}= 1-10$  μm).

CuO and  $Cu_2O$  are characterized as non-toxic materials that are available, inexpensive and have a high absorption coefficient in the visible range [40]. J. Türk et al. conducted experimental studies and obtained good results for p-i-n CdTe solar cell with a conversion efficiency of 15.21% [41], using copper oxide as a back contact. These results indicate that CuO and  $Cu_2O$  materials can be used to increase the efficiency of CdTe solar cells.

Therefore next material used was copper oxide CuO with a band gap of ~ 1.51 eV. The thickness of the back contact varied in the range 1-10 μm with step of 1 μm.

In this study a simulation of the back contact layer of thin-film CdTe solar cells using CuO and  $Cu_2O$  materials were conducted. In particular, it was found that the material of the back contact affects the efficiency of the final cell, but the obtained data for  $Cu_2O$  as a back contact material have shown that adding of this layer did

not significantly increase the efficiency of the final cell due to the energy difference of the band gap at the transition CdTe/Cu<sub>2</sub>O [39]. Accordingly, it was decided to add a layer of CuO.

The authors performed simulations for defect free ZnO/CdS/CdTe/CuO heterostructure and the results of the simulation are shown in Fig. 9. The layer thicknesses of CdTe, CdS and ZnO were set to 3 μm, 50 nm and 50 nm respectively, while the thickness of CuO contact layer was 5 μm.

The best value of efficiency was obtained at a thickness of a back contact of 5 μm and is ~ 20,94%.

## Conclusions

1. Numerical simulations of the efficiency of photovoltaic cell with variation in thickness of individual layers were performed using SCAPS software to analyze the semiconductor properties that affect the efficiency of solar cells based on CdTe.

2. The values of photoelectric efficiency for thin-film heterostructural solar cells ZnO/CdS/CdTe and ZnO/CdS/CdTe/CuO 19.22% and 20.94%, respectively, were obtained. The optimal layers thicknesses of CdTe, CdS, ZnO, and CuO were set to 3 μm, 50 nm, 50 nm, and 5 μm, respectively.

3. Among the properties of thin films, the simulation results suggested that the thickness of the window layer and the absorber layer more significantly affect the value of the short-circuit current density and the efficiency of solar cells based on CdTe.

**Zapukhlyak Z.R.** – PhD Student, Department of Physics and Chemistry of Solids;

**Nykyruy L.I.** – Ph.D, Prof., Department of Physics and Chemistry of Solids;

**Rubish V.M.** – Ph.D., Prof., Head of the Uzhhorod Laboratory of Optoelectronics and Photonics Materials;

**Wisz G.** – Ph.D, Prof., Department of Experimental Physics;

**Prokopiv V.V.** – Ph.D, Prof., Head of the Department of Physics and Chemistry of Solids;

**Galushchak M.O.** – Dr. Sc., Prof., Head of the Department of General and Applied Physics;

**Lishchynskyy I.M.** – Ph.D, Assoc. Prof., Head of the Department of Physics and Methods of Teaching;

**Katanova L.O.** – student of Physical-Technical Faculty;

**Yavorskyi R.S.** – Ph.D., Department of Physics and Chemistry of Solids.

- [1] B.K. Ghosh, I. Saad, K.T.K. Teo, and S.K. Ghosh, *Optik* 206, 164278 (2020) (<https://doi.org/10.1016/j.ijleo.2020.164278>).
- [2] G. Wisz, L.I. Nykyruy, V.M. Yakubiv, I.I. Hryhoruk, R.S. Yavorskyi, *International Journal of Renewable Energy Research* 8(4), 2367 (2018).
- [3] R.Y. Petrus, H.A. Ilchuk, A.I. Kashuba, et al., *Journal of Applied Spectroscopy* 87(1), 35 (2020) (<https://doi.org/10.1007/s10812-020-00959-7>).
- [4] J.M. Kephart, R.M. Geisthardt et al., *Prog. Photovolt: Res. Appl.* 23, 1484 (2015) (<https://doi.org/10.1002/pip.2578>).
- [5] Web-source: <https://www.nrel.gov/pv/cell-efficiency.html>.
- [6] S. Marjani, S. Khosroabadi, and M. Sabaghi, *Optics & Photonics Journal* 6(2), 15 (2016) (<http://dx.doi.org/10.4236/opj.2016.62003>).
- [7] S.G. Kumar, K.K. Rao, *Energy & Environmental Science* 7(1), 45 (2014) (<https://doi.org/10.1039/C3EE41981A>).
- [8] E. Colegrove, R. Banai, C. Blissett, C. Buurma, J. Ellsworth, *Journal of Electronic Materials* 41, 2833 (2012) (<https://doi.org/10.1007/s11664-012-2100-z>).
- [9] A.B. Danylov, H.A. Ilchuk, R.Yu. Petrus, *Acta Physica Polonica A* 133(4), 981 (2018).
- [10] M.A. Green, K. Emery, Y. Hishikawa, W. Warta, *Progress in photovoltaics* 19(1), 84 (2011) (<https://doi.org/10.1002/pip.1088>).
- [11] M.A. Green, E.D. Dunlop, J. Hohl-Ebinger, M. Yoshita, N. Kopidakis, X. Hao, *Progress in Photovoltaics: Research and Applications* 28(7), 629 (2020) (<https://doi.org/10.1002/pip.3303>).
- [12] R. Naba, Paudela, Y. F. Yan, *Applied Physics Letters* 105, 183510 (2014) (<https://doi.org/10.1063/1.4901532>).
- [13] F. Anwar, S. Afrin, S.S. Satter, R. Mahbub, S.M. Ulah, *Journal of Renewable Energy Research* 7(2), 885 (2017).
- [14] A. Haddout, A. Raidou, M. Fahoume, *Optoelectronics Letters* 14, 98 (2018) (<https://doi.org/10.1007/s11801-018-7229-4>).
- [15] S.M. Seck, E.N. Ndiaye, M. Fall, S. Charvet, *Natural Resources* 11(4), 147 (2020) (<https://doi.org/10.4236/nr.2020.114009>).
- [16] O. Shoewu, G. Anuforonini, O. Duduyemi, *Review of Information Engineering & Applications* 3(1), 1 (2016) (<https://doi.org/10.18488/journal.79/2016.3.1/79.1.1.10>).
- [17] R. Yavorskyi, et al., *Applied Nanoscience* 9(5), 715 (2019) (<https://doi.org/10.1007/s13204-018-0872-z>).



- [18] R. Yavorskyi, *Physics and Chemistry of Solid State* 21(2), 243 (2020) (<https://doi.org/10.15330/pcss.21.2.243-253>).
- [19] L.I. Nykyruy, R.S. Yavorskyi, Z.R. Zapukhlyak, G. Wisz, and P. Potera, *Optical Materials* 92, 319 (2019) (<https://doi.org/10.1016/j.optmat.2019.04.029>).
- [20] L. Nykyruy, Y. Saliy, R. Yavorskyi, Y. Yavorskyi, V. Schenderovsky, G. Wisz, & S. Górný, CdTe vapor phase condensates on (100) Si and glass for solar cells. In 2017 IEEE 7th International Conference Nanomaterials: Application & Properties (NAP) 01PCSI26-1, IEEE (2017) (<https://doi.org/10.1109/NAP.2017.8190161>).
- [21] A. Morales-Acevedo, N. Hernández-Como, G. Casados-Cruz, *Mater. Sci. Eng. B* 177(16), 1430 (2012) (<https://doi.org/10.1016/j.mseb.2012.01.010>).
- [22] D. Wang, H. Cui, G. Su, *Sol. Energy* 120, 505 (2015) (<https://doi.org/10.1016/j.solener.2015.07.051>).
- [23] M. Burgelman, J. Verschraegen, S. Degrave, P. Nollet, *Prog. Photovoltaics Res. Appl.* 12(2-3), 143 (2004) (<https://doi.org/10.1002/pip.524>).
- [24] M. Burgelman, P. Nollet, S. Degrave, *Thin Solid Films* 361, 527 (2000) ([https://doi.org/10.1016/S0040-6090\(99\)00825-1](https://doi.org/10.1016/S0040-6090(99)00825-1)).
- [25] M. Burgelman, J. Marlein, Analysis of graded band gap solar cells with SCAPS, *Proc. Of the 23rd Eur. Photovolt. Sol. Energy Conf., Valencia*, 2151–2155 (2008) (<https://doi.org/10.1854/LU-678258>).
- [26] J. Verschraegen, M. Burgelman, *Thin Solid Films* 515(15), 6276 (2007) (<https://doi.org/10.1016/j.tsf.2006.12.049>).
- [27] S. Degrave, M. Burgelman, P. Nollet, Modelling of polycrystalline thin film solar cells: new features in SCAPS version 2.3, *Proc. Of 3<sup>rd</sup> World Conf. on Photovolt. Energy Convers*, vol 1, 487–490 (2003) (ISBN:4-9901816-0-3).
- [28] M. Gloeckler, A.L. Fahrenbruch, J.R. Sites, Numerical modeling of CIGS and CdTe solar cells: setting the baseline, *Proc. Of 3<sup>rd</sup> World Conf. on Photovolt. Energy Convers*, vol 1, 491–494 (2003).
- [29] G. Heal, *Reflections – the Economics of Renewable Energy in the United States*, Review of Environmental Economics and Policy. Oxford University Press for Association of Environmental and Resource Economists 4(1), 139-154 (2010). (<https://www.nber.org/papers/w15081.pdf>).
- [30] M. Gloeckler, A. L. Fahrenbruch, J. R. Sites, Numerical modeling of CIGS and CdTe solar cells: setting the baseline. *Proc. of 3<sup>rd</sup> World Conf. on Photovolt. Energy Convers.*, 1, 491-494 (2003).
- [31] H. Zerfaoui, D. Dib, M. Rahmani, K. Benyelloul, C. Mebarkia, Study by simulation of the SnO<sub>2</sub> and ZnO anti-reflection layers in n-SiC/p-SiC solar cells. In *AIP Conf. Proc.*, 1758(1), 030029 (2016) (<https://doi.org/10.1063/1.4959425>).
- [32] C. Dumitrache, N. Olariu, E. St. Lakatos, G. Mantescu, L. Olteanu, M. Badea, *Electrotehnica Electronica Automatica* 61(1), 25 (2013).
- [33] S. Khosroabadi, S. H. Keshmiri, *Opt. Expr.* 22(103), A921 (2014) (<https://doi.org/10.1364/OE.22.00A921>).
- [34] N. Amin, K. Sopian, M. Konagai, *Sol. Energy Mater. and Sol. Cells* 91(13), 1202 (2007) (<https://doi.org/10.1016/j.solmat.2007.04.006>).
- [35] P. Sawicka-Chudy, Z. Starowicz, G. Wisz, R. Yavorskyi, Z. Zapukhlyak, M. Bester, M. Sibiński, M. Cholewa, *Materials Research Express* 6(8), 085918 (2019) (<https://doi.org/10.1088/2053-1591/ab22aa>).
- [36] G.A. Il'chuk, V.V. Kusnezh, V.Y. Rud', et al., *Semiconductors* 44(3), 318 (2010) (<https://doi.org/10.1134/S1063782610030085>).
- [37] J. Türck, H.J. Nonnenmacher, P.M. Connor, S. Siol, B. Siepchen, J.P. Heimfarth, A. Klein, W. Jaegermann, *Prog. Photovoltaics Res. Appl.* 24, 1229 (2016) (<https://doi.org/10.1002/pip.2782>).
- [38] G. Wisz, P. Sawicka-Chudy, P. Potera, M. Sibiński, R. Yavorskyi, Ł. Głowa, B. Cieniek, M. Cholewa, *Molecular Crystals and Liquid Crystals* 672(1), 81 (2018) (<https://doi.org/10.1080/15421406.2018.1542110>).
- [39] P. Sawicka-Chudy, M. Sibiński, E. Rybak-Wilusz, M. Cholewa, G. Wisz, R. Yavorskyi, *AIP Advances* 10(1), 010701 (2020) (<https://doi.org/10.1063/1.5125433>).
- [40] P.D. DeMoulin, M.S. Lundstrom, *IEEE Trans. Electron. Dev.*, 36, 897 (1989) (<https://doi.org/10.1109/16.299671>).
- [41] W. Zhang, Y. Li, S. Zhu, F. Wang, *Surf. Coat. Technol.* 182(2-3), 192 (2004) (<https://doi.org/10.1016/j.surfcoat.2003.08.050>).



Ж.Р. Запукхляк<sup>1</sup>, Л.І. Никируй<sup>1</sup>, В.М. Рубіш<sup>2</sup>, Г. Віш<sup>3</sup>, В.В. Прокопів<sup>1</sup>,  
М.О. Галушак<sup>4</sup>, І.М. Ліщинський<sup>1</sup>, Л.О. Катанова<sup>1</sup>, Р.С. Яворський<sup>1</sup>

## **SCAPS моделювання гетероструктури ZnO/CdS/CdTe/CuO для застосування у фотоелектричних перетворювачах**

<sup>1</sup>Прикарпатський національний університет імені Василя Стефаника, Івано-Франківськ, Україна,  
[zhanna.zapukhlyak@gmail.com](mailto:zhanna.zapukhlyak@gmail.com)

<sup>2</sup>Ужгородська лабораторія Інституту реєстрації інформації НАН України, Ужгород, Україна

<sup>3</sup>Жешувський університет, Жешув, Польща,

<sup>4</sup>Івано-Франківський національний технічний університет нафти і газу, Івано-Франківськ, Україна

У середовищі комп'ютерних симуляцій фотоелектричних комірок SCAPS (Solar Cell Capacitance Simulator) виконано комплексне моделювання оптичних та фотоелектричних властивостей комірки на основі гетероструктури ZnO/CdS/CdTe/CuO. Обґрунтовано вибір високорезистивного прозорого (HRT) оксидного матеріалу - для використання у якості фронтального контакту. Досліджено вплив товщини плівки на ефективність кінцевої комірки. Ефективність розглядуваної фотоелектричної комірки склала 20,94%. Структуру фотоелектричної комірки обирали, виходячи із аналізу властивостей окремих шарів із товщиною. При цьому, додаючи кожен наступний шар, переглядалися властивості гетеросистеми. Таким чином, підібрано оптимальні товщини фотоелектричної гетеросистеми, які дозволяють отримати максимальну ефективність. Моделювання базувалося на основі експериментальних даних (товщина, оптичні характеристики, ширина забороненої зони) для кожної із плівкових систем, отриманих методом фізичного осадження у вакуумі (PVD).

**Ключові слова:** тонкі плівки, фотоелектрика, CdTe, гетероструктура ZnO/CdS/CdTe/CuO, сонячні елементи, моделювання SCAPS.